HHS Public Access

Author manuscript

Radiat Res. Author manuscript; available in PMC 2016 April 01.

Published in final edited form as:

Radiat Res. 2015 April ; 183(4): 398–406. doi:10.1667/RR13916.1.

Type 2 Diabetes is a Delayed Late Effect of Whole-Body Irradiation in Nonhuman Primates

Kylie Kavanagh, **Michael D. Dendinger**, **Ashley T. Davis**, **Thomas C. Register**, **Ryne DeBo**, **Greg Dugan**, and **J. Mark Cline**[1]

Wake Forest School of Medicine, Department of Pathology, Winston-Salem, North Carolina

Abstract

One newly recognized consequence of radiation exposure may be the delayed development of diabetes and metabolic disease. We document the development of type 2 diabetes in a unique nonhuman primate cohort of monkeys that were whole-body irradiated with high doses (6.5–8.4 Gy) 5–9 years earlier. We report here a higher prevalence of type 2 diabetes in irradiated monkeys compared to age-matched nonirradiated monkeys. These irradiated diabetic primates demonstrate insulin resistance and hypertriglyceridemia, however, they lack the typical obese presentation of primate midlife diabetogenesis. Surprisingly, body composition analyses by computed tomography indicated that prior irradiation led to a specific loss of visceral fat mass. Prior irradiation led to reductions in insulin signaling effectiveness in skeletal muscle and higher monocyte chemoattractant protein 1 levels, indicative of increased inflammation. However, there was an absence of large defects in pancreatic function with radiation exposure, which has been documented previously in animal and human studies. Monkeys that remained healthy and did not become diabetic in the years after irradiation were significantly leaner and smaller, and were generally smaller and younger at the time of exposure. Irradiation also resulted in smaller stature in both diabetic and nondiabetic monkeys, compared to nonirradiated age-matched controls. Our study demonstrates that diabetogenesis postirradiation is not a consequence of disrupted adipose accumulation (generalized or in ectopic depots), nor generalized pancreatic failure, but suggests that peripheral tissues such as the musculature are impaired in their response to insulin exposure. Ongoing inflammation in these animals appears to be a consequence of radiation exposure and can interfere with insulin signaling. The reasons that some animals remain protected from diabetes as a late effect of irradiation are not clear, but may be related to body size. The translational relevance for these results suggest that muscle may be an important and underappreciated target organ for the delayed late effect of whole-body irradiation, leading to increased risk of insulin resistance and diabetes development.

INTRODUCTION

Individuals who survive the initial acute effects of radiation therapy may also be faced with the added burden of additional adverse delayed late effects, which are still being discovered

[1]Address for correspondence: Department of Pathology, Section on Comparative Medicine, Wake Forest University Health Sciences, Medical Center Blvd., Winston-Salem, NC 27127; jmcline@wakehealth.edu.

and characterized by researchers. One of the more recently recognized consequence postirradiation may be the development of diabetes and metabolic disease, which has been documented in some childhood and adult cancer survivors (1, 2). Controversy still exists as to whether this increase in risk is truly present in human populations exposed to ionizing radiation through cancer therapy or other exposures (3). However, in a recent publication, type 2 diabetes mellitus (T2DM) hospitalization rates for survivors of childhood cancer were reported to be 1.6-fold greater than the rates seen in age-matched cohorts at all time points after successful cancer treatment (1). A smaller clinical study (4) supports this finding with a disease prevalence of 7.8% in patients with prior cancer therapy compared to 4.5% in patients not exposed to radiation therapy and 42% of the attributable risk for diabetes could be accounted for by cancer therapy. This rate is remarkably close to the 8.3% incidence rate seen in adults, 20 years after abdominal radiation therapy for Hodgkin lymphoma (2). In a study on childhood cancer survivors (1), the researchers found that hospitalization rates for diabetes increased as time since radiotherapy increased. What is particularly interesting is that the risk of T2DM development appears to be higher than type 1 diabetes mellitus (T1DM) after radiation therapy for most tumor types. Whereas T1DM represents the failure of the pancreas to produce and release adequate insulin, T2DM generally features peripheral tissue insulin resistance in combination with dysfunctional pancreatic responses to hyperglycemia. The higher prevalence of T2DM supports a potentially important role for peripheral tissues in diabetes mellitus (DM) disease development. Clinical studies do not easily allow for the relative contributions of radiation and chemotherapeutic exposures in metabolic disease development, and thus preclinical animal evaluations of radiation exposure are important to inform physicians and scientists.

High-dose whole-body irradiation (WBI) (8– 10 Gy cumulatively) injures beta cells and impairs insulin responses to glucose challenge in monkeys in the short term (5), however, less is known about the effects on the important muscle, liver and fat tissues that are involved in glucose disposal (6), production and inflammation, respectively. In the current study, we show the characteristics of a nonhuman primate cohort of monkeys that had been exposed to high-dose radiation 5–9 years earlier and compare these to age-matched nonirradiated monkeys. We focused on evaluations of body composition and characterization of insulin action. By understanding the mechanisms underlying radiation-induced metabolic disease development, efforts can be focused on potential approaches for prevention and treatment, and identifying those patients who are at greater risk for developing this late effect.

METHODS

Animals

A cohort of 34 adult male rhesus macaques were sourced from the University of Maryland (College Park, MD), the Armed Forces Radiobiology Research Institute (Bethesda, MD) and the University of Illinois at Chicago (Chicago, IL). The animals were moved to Wake Forest School of Medicine (WFSM) as part of the animal core within the Radiation Countermeasures Centers of Research Excellence (RadCCORE) consortium to collectively and collaboratively develop agents that detect and mitigate radiation exposure and provide

acute treatment for people who have been exposed to deterministic doses of radiation (www.radccore.org/).

The animals used in our study are survivors of a single sublethal WBI dose (6.5–8.4 Gy) 5–9 years prior to this study (Table 1). Exposures in this range are expected to have <5% mortality (7). A group of age-matched male nonirradiated monkeys were additionally sourced and moved to WFSM. Prior to arrival at WFSM, animals were fed standard laboratory chow diets containing 18% protein, 13% fat and 69% carbohydrates (Monkey Diet 5038; LabDiet®, St. Louis, MO). In 2010, animals were transitioned to a diet comparable to that consumed by a typical North American, containing 18.4% protein, 36.6% fat and 45% carbohydrates (Monkey Diet 5L0P). A subset of monkeys were observed to develop diabetes, defined as having a fasting glucose concentration over 126 mg/dL or a glycation of hemoglobin chain A1c (HbA1c) of greater than 6.5%. These monkeys were transitioned back to the laboratory chow diet because it is higher in fiber with a very low glycemic index. Insulin therapy was initiated as twice-daily insulin injections [70% intermediate-acting (NPH), 30% short-acting (regular insulin) Novolin® 70/30; Novo Nordisk, Inc., Princeton, NJ]. Insulin doses were adjusted based on whole blood glucose measurements determined by glucometer approximately 3–4 h after insulin dosing and feeding (postprandial) at least twice weekly. All monkeys were given access to supplemental fresh fruits and vegetables daily. Animals that died during the study underwent a complete necropsy by a board-certified veterinary pathologist (JMC), with standard histopathological examinations of tissues. All animal procedures were performed according to the protocol approved by the Wake Forest University Institutional Animal Care and Use Committee according to recommendations in the Guide for Care and Use of Laboratory Animals (Institute for Laboratory Animal Research) and in compliance with the USDA Animal Welfare Act and Animal Welfare Regulations (Animal Welfare Act as Amended; Animal Welfare Regulations).

Study Design

All monkeys had general health assessments that included metabolic health assessments, body composition analysis and vascular stiffness assessments. A subset of animals (n = 6 per group) from the nonirradiated controls (NonRad-CTL), irradiated nondiabetic (Rad- CTL) and irradiated diabetic (Rad-DM) monkeys were further characterized for glucose metabolism and circulating inflammatory end points described below.

Blood parameters—Monkeys determined to have diabetes had all combination insulin administration withdrawn for at least 24 h and regular insulin withdrawn for at least 12 h prior to assessment. All monkeys were fasted for a minimum of 12 h prior to assessment, and animals anesthetized with intramuscular ketamine (10–15 mg/kg) to allow for sample and data collection. Each animal was weighed, and blood samples were obtained by venipuncture of the femoral vein and collected into ethylenediaminetetraacetic acid and serum separator blood tubes. The blood samples were placed on ice until processed, after which the plasma and whole blood samples were stored at −80°C until analysis. Fasting blood glucose was determined by the glucose oxidase method, and fasting plasma insulin concentration was determined by enzyme linked immunosorbent assay (ELISA) (Mercodia,

Uppsala, Sweden) from the plasma sample. Homeostasis model assessment (HOMA) was determined by the product of glucose and insulin divided by 22.5 and used to evaluate insulin resistance (8). Whole blood was used to determine the HbA1c using HPLC methodology (Primus PDQ, Primus Diagnostics, Kansas City, MO). Triglyceride (TG), high-density lipoprotein cholesterol (HDLc) and total plasma cholesterol (TPC) concentrations were measured enzymatically. In the cohort of monkeys evaluated for insulin sensitivity, additional circulating concentrations of interleukin-6 (IL-6), monocyte chemoattractant protein 1 (MCP-1) (R&D Systems™, Minneapolis, MN) and C-reactive protein (CRP) (ALPCO® Diagnostics, Salem, NH) were measured by ELISA. Waist circumference was measured and body mass index calculated, using the crown-rump length rather than total height. Trunk length was measured from the suprasternal notch to the pubic symphysis using an electronic caliper.

Insulin sensitivity—Insulin sensitivity was additionally assessed in 6 monkeys from the NonRad-CTL, Rad-DM and Rad-CTL groups by glucose and meal tolerance testing (GTT and MTT, respectively), and insulin-stimulated muscle biopsy with quantification of the activation of insulin receptor substrate 1 (IRS-1) and Akt. For the GTT, a temporary peripheral intravenous catheter was used to infuse 50% dextrose (500 mg/kg) via the saphenous vein, followed by saline flush. Blood samples were subsequently collected at 2, 3, 5, 8, 10, 20, 30 and 60 min post-dextrose into EDTA-treated tubes and placed on ice. Samples were centrifuged, and the plasma was stored at −80°C until analysis for glucose and insulin concentrations. The rate of glucose clearance was calculated as the slope of the log transformed glucose values between 5 and 20 min. Areas under the glucose and insulin curve (AUCs) were calculated using the trapezoidal method. The acute insulin response (AIR) was calculated as the average of 5 and 10 min insulin concentrations, and a disposition index (DI) was calculated from the maximal glucose excursion divided by AIR. MTT was achieved by gavage with a meal replacement solution (71% of calories supplied as carbohydrate, 11% from protein and 17% from fat) at 10% of their daily caloric requirement and blood samples were collected at 15, 30, 60, 90 and 120 min post-feeding. AUCs for insulin and glucose were calculated from the resultant data.

Biopsies were collected under baseline and then insulin-stimulated conditions. Regular insulin was infused into a peripheral vein at 40 U/m^2/min for 15 min, predicted to increase the average circulating insulin concentration to 100 μIU/ml (9). A muscle biopsy sample was collected during the insulin infusion, frozen in liquid nitrogen and stored at −80°C until analysis. Protein was extracted from biopsy samples and analyzed for total and phosphorylated (activated) IRS-1 and Akt levels by ELISA according to manufacturer recommendations (Biosource, Camarillo, CA). Data are reported as the percentage of total protein activated with insulin.

Pulse wave velocity—Blood pressure [systolic and diastolic blood pressure (SBP and DBP, respectively)] was measured indirectly at the tail base. Vascular stiffness was measured by brachial-femoral pulse wave velocity using automated methods (SphygmoCor; Atcor Medical Inc., Itasca, IL).

Body composition—Computed tomography (CT) was used to estimate fat and lean tissue volume for the entire monkey and for defined hind limb sections. Scans were performed on a Toshiba 32-slice Aquilion scanner (Toshiba America Medical Systems, Tustin, CA). The CT images were reconstructed with TeraRecon Aquarius Intuition software (TeraRecon, Foster City, CA). Thresholds of − 140 to − 40 Hounsfield units (HU) were used to define the fat-containing voxels and thresholds of − 5 to − 135 HU were used to define lean tissue. Fat mass was calculated from volume results (corrected for fat density of 0.918 g/cm^3) and expressed as a percentage of the animal's total body weight. Lean tissue was similarly calculated from volume results (corrected for muscle density of 1.055 g/cm^3). Additionally, hind limb muscle mass and composition were separately estimated by applying thresholds for muscle and fat for only image slices distal to the sacroiliac joint. Similarly, abdominal fat distribution into intraabdominal or subcutaneous fat compartments was assessed by limiting analysis to the region between the thoracolumbar junction and pubic symphysis using automated differentiation of depots within and outside the body wall. Fat mass and ratios for this body region were calculated after correction for tissue density. Average CT attenuation values were collected for liver and skeletal muscle, by triplicate measures of regions of interest (ROI) placed over homogenous sections of liver and duplicate ROIs over the belly of both quadriceps muscles (calculated as the slice midway between the patellar and pubic symphysis).

Data Analysis

Data was log transformed as required to achieve statistical assumptions of normality. Data is expressed throughout as means ± standard error of the mean. Group differences were analyzed using one-way analysis of variance (ANOVA) with alpha level set at 0.05 for statistical significance and then additionally examined for the effect of radiation by ANOVA. Body composition measures were covaried by the monkey's age at assessment. Post-hoc analyses were conducted using Tukey's honest significant differences testing. Correlation coefficients were determined by Pearson's *r* statistics for association. All statistical testing was performed using Statistica V10 (StatSoft Inc., Carlsbad, CA).

RESULTS

Within the irradiated cohort (n = 22), 9 monkeys had significant metabolic disease classified as prediabetes or diabetes (fasting glucose > 100 mg/dL) compared to 0 monkeys within the age-matched control group (n = 12). Table 1 describes the basic demographic, cardiometabolic and inflammatory characteristics of these monkeys. The irradiated monkeys that became diabetic did not differ in terms of how much time had elapsed after exposure or age (Table 1), but actually had lower total radiation exposure than the irradiated nondiabetic monkeys. The initial onset of T2DM after irradiation ranged from 4 to 10.5 years, with an average delay of 6 years (±0.77). Diabetic monkeys had higher glucose and TG values, and the inflammatory marker MCP-1 was higher in the irradiated monkeys as a group. No changes in cardiovascular parameters were noted (Table 1) aside from a trend for irradiated monkeys to have higher heart rates ($P = 0.09$).

Another characteristic of the Rad-DM monkeys was that body weight and body composition departed from the overweight or obese state that is normally associated with type 2 DM (Fig. 1A). The Rad-DM monkeys were of comparable weight to the NonRad-CTL monkeys, not heavier as is typical, and the Rad-CTL monkeys were >40% leaner than the age-matched NonRad-CTL and Rad-DM animals. Specifically, the Rad-CTL animals had lower total body fat, and higher proportions of lean tissue, including a significantly more dense liver parenchyma as shown by CT (Table 2), which indicates a lower liver fat content. All of these outcomes indicate a healthier state in the Rad-CTL group. The Rad-DM monkeys had body compositions indistinguishable from age-matched NonRad-CTL animals. Even more surprising was the finding of a significant reduction in visceral fat with radiation exposure (Fig. 1B). Further, a significant association between radiation dose and visceral fat was seen ($r = -0.52$, $P = 0.0030$), i.e., the higher the radiation dose, the greater the loss of visceral fat. These alterations in body composition were verified by analysis of CT scans from the prior year, where the same changes were observed (data not shown). Radiation exposure also had a significant negative effect on stature, as measured by trunk length (Table 1), leading to a 7% shortening measurable many years after radiation exposure.

A trend was observed where the Rad-DM monkeys had more subcutaneous fat in their midsection while the Rad-CTL monkeys had less ($P = 0.09$). Other body composition end points measured by CT supported the pattern that the Rad-DM animals were comparable to the NonRad-CTL animals and the Rad-CTL animals were leaner. We examined the body weight at the time of irradiation, and a trend was apparent ($P = 0.10$) for larger animals to become diabetic in the future compared to smaller animals (Fig. 1C). This difference in size could relate to small differences in age and developmental stage at the time of exposure. The age range at exposure was 3–9 years for both groups and did include monkeys likely prepubescent and not fully mature (<4 years). In the Rad-DM group 37.5% were potentially prepubertal at exposure, while 69% of the Rad-CTL group were prepubertal, suggesting that younger monkeys may respond to radiation differently.

The Rad-DM monkeys were hyperglycemic and relatively hyperinsulinemic, with variability in insulin values related to whether monkeys were still overproducing insulin to compensate for peripheral insulin resistance, or had become hypoinsulinemic with pancreatic exhaustion, both of which are associated with impaired glycemic control (Table 1; Fig. 2A and B). The diagnosis of T2DM was generally supported by histopathologic assessments of pancreata from the Rad-DM monkeys that died, with 2 of the 3 animals demonstrating amyloid accumulation in the pancreatic islets (Fig. 2C).

Dynamic assessments of insulin sensitivity, using meal and glucose tolerance testing, confirmed that the Rad-CTL monkeys had no overt metabolic or pancreatic defects under relatively normal challenge conditions (Fig. 3). Acute insulin response (phase 1 secretion) and disposition index did not differ among groups, however, glucose disposal rates (calculated K values) tended to be impaired in the Rad-DM monkeys, at 40% lower than both the Rad-CTL and NonRad-CTL groups ($P = 0.15$; Table 3). Interestingly, when skeletal muscle insulin sensitivity was assessed under supraphysiological conditions of circulating insulin, significantly reduced insulin signaling ability was observed in irradiated monkeys as assessed by Akt ($P = 0.03$), as well as a trend for reduced IRS-1 activation ($P =$

0.06) even in the absence of frank diabetes mellitus (Fig. 4). Rad-DM monkeys had approximately half the signaling effectiveness, whereas Rad-CTL monkeys that were metabolically normal had intermediate values (nonsignificantly reduced) with 27% and 18% reduction in IRS-1 and Akt activations, respectively. There were no group differences in total IRS-1 or Akt abundance ($P > 0.05$ for both, data not shown). These differences in insulin-stimulated activations may be dependent on inflammatory processes (Table 1). MCP-1 did show an increase with radiation exposure and highest values in the Rad-DM monkeys, but no changes in CRP or IL-6 were observed, potentially due to the small size of the cohort (n =6/group) examined for these end points.

DISCUSSION

The late development of diabetes mellitus in response to whole-body irradiation in a NHP model is a novel observation. In this study, we showed that type 2 diabetes developed many years after irradiation in a selected population, however, traditional risk factors for diabetes such as visceral and ectopic fat deposition were absent (10, 11). In fact, radiation exposure was associated with a loss of abdominal fat, and the irradiated monkeys that did not develop diabetes were significantly leaner than either age-matched control or irradiated diabetic monkeys. They also had higher attenuation of CT X rays in tissues assessed (liver and muscle) consistent with greater tissue density, which is often interpreted as containing less lipid (12). These differences in body composition, and perhaps the metabolic consequences, may have their origins in age and size at the time of exposure. Slightly smaller, younger monkeys remained nondiabetic, lean and healthy postirradiation, which may reflect a growth retardation effect that is known to occur in children (13). This effect was seen in our study animals, with reductions in stature observed in both the diabetic and nondiabetic groups of irradiated monkeys. In many animal models a smaller size is associated with improved insulin sensitivity and longevity related to lower insulin signaling through both lower circulating insulin and insulin-like growth factors (IGF) (14, 15). The differences in age and associated weight observed here are too small to serve as a practical or useful tool for risk assessment of future diabetogenesis in exposed people. These monkeys are not the first animal model to dissociate ectopic fat accumulation and insulin sensitivity. Although less common phenotypes, abdominally lean insulin-resistant mice have been generated with genetic manipulation of the insulin-like growth factor 1(IGF-1) receptor, and hibernating bears are obese and insulin sensitive (16–18).

The Third National Health and Nutrition Examination Survey reported that skeletal muscle index was related to insulin sensitivity in midlife adults, even after adjusting for obesity measures and age (19). The amount of muscle mass is an important determinant in glucose disposal, since muscle metabolizes approximately 90% of circulating glucose (6), however, our nondiabetic monkey groups differed in muscle mass, but not necessarily glucose disposal. Differences in glycemic control related to muscle are likely to reflect both muscle metabolic function (20) as well as myocyte mass. We observed that irradiated monkeys had impaired muscle responses to insulin, suggesting the primary defect is post-insulin receptor binding. It is biologically relevant that there was intermediate ability of irradiated nondiabetic monkeys to respond to insulin. Where healthy irradiated nondiabetic monkeys had impaired insulin effectiveness, they had adequate muscle mass (relatively more than

age-matched control monkeys), lower fat mass and were able to maintain glycemic control. It is likely with larger sample sizes that the trend for irradiated nondiabetic monkeys would become stronger, and suggests skeletal muscle is a peripheral tissue target organ for the development of diabetes as a late effect of radiation exposure. One open question that results from these findings is whether increased adiposity in the currently healthy irradiated nondiabetic monkeys would promote insulin resistance.

Common mechanisms of peripheral tissue insulin resistance include inflammatory signaling, which causes activation of c-Jun-N-terminal kinase, which in turn is able to serine-phosphorylate the insulin receptor and reduce its activity (21). A survey of inflammatory end points demonstrated elevations in MCP-1 in irradiated animals, which supported an inflammatory basis for the reduced insulin signaling effectiveness. Fibrosis is a well recognized consequence of radiation exposure and a nonreversible process (22, 23). Fibrosis is the excessive accumulation of collagen and other extracellular matrix (ECM) components and is characterized by an imbalance between breakdown and synthesis of ECM components. The vascular endothelium is a particularly important target cell, because damage leads to inflammation and reduced perfusion, and thus progression of both the fibrotic response and reduced ability to clear and respond to circulating insulin (24, 25). Muscle fibrosis is a delayed late effect of radiation and is associated with tissue atrophy (22). We did not see a radiation effect on the amounts of total lean tissue or leg lean tissue, which is predominantly muscle. However, fibrosis may exist without atrophy, and characterization of the ECM will be the focus of future assessments in these animals.

Our cardiovascular assessments included brachial-tofemoral artery vascular stiffness, which is a surrogate marker of mostly aortic fibrosis and did not elucidate any large vessel compromise. Blood pressure equivalency also suggests no difference in smaller vessels.

Prior WBI animal studies have documented consistent effects on the pancreas. Short-term studies in baboons have shown morphologic changes to the pancreas and necrosis of pancreatic islet cells and acinar tissue (5). Pancreatic atrophy and exocrine pancreatic insufficiency in response to irradiation have been reported in dog models (26, 27). Our study differs in that we are examining pancreatic function many years postirradiation, and our animals consumed a Western diet high in saturated fat and simple sugar, which both challenge endocrine pancreatic function and promote glucolipotoxicity, leading to beta cell dysfunction and eventual death (28, 29). In the irradiated diabetic monkeys, aside from a trend towards fasting hyperinsulinemia, we saw no large differences in pancreatic function in response to glucose or a mixed meal. However, large variability exists within the diabetic cohort as illustrated by the presence and absence of pancreatic amyloid in irradiated diabetic monkeys and a broad range of HOMA scores for insulin resistance. The inadequate insulin secretion from the pancreas and cellular response at the level of muscle (and possibly other peripheral tissues) likely contribute in an additive manner to the lack of normal glucose disposal (evidenced by elevated HbA1c values and slow glucose disappearance).

The strengths of our study include the use of the unique resource of irradiated nonhuman primates that are available many years after exposure for study. Nonhuman primates are preferred to rodent models since their tissue architectures, inflammatory and immune

responses resemble that of humans (30–32). Of particular relevance to the current study, the concordance with humans of relative abundance of slow and fast twitch muscle fiber types has implications for muscular metabolic capacity (33). Diabetogenesis as a late effect of radiation exposure has significant public health implications with the increasing use of therapeutic radiation and potential large-scale malicious exposures, and monkeys are an optimal model for spontaneous T2DM (34–37). Naturally occurring diabetes is not typically seen in rodents without genetic manipulation, in part because rodents have inherently higher beta cell regeneration rates compared to monkeys and humans (38). The monkeys in our study also consume a diet comparable to people in westernized nations, and so their tissues are challenged and adipogenesis is promoted as in the clinical population, which increases the translatability of our findings.

Our study also has some limitations. Small sample size may have limited the ability to statistically define differences between groups, despite biological differences likely being present. Our cohort represents WBI survivors, even though doses were sublethal (7), and may possess some survival-related phenotypes not present across the whole population, thus may be particularly relevant to humans who survive to develop delayed late effects of radiation. Our monkey cohort is comprised of animals from multiple institutions with variable environments that may have influenced disease risk. The average age of T2DM diagnosis was 19 years, with the youngest onset of diabetes reported at 10 years old in a large T2DM rhesus macaque colony (39). Our monkeys were on average 11.5 years old and thus diabetes prevalence would be expected to be very low. This is reflected in the nonirradiated control group, which had 0% prevalence, and is in contrast to nearly 30% prevalence in the irradiated monkeys, thus illustrating the excess risk of disease at this age with exposure.

The monkeys in our study demonstrate that prior WBI leads to increased incidence of diabetes years after exposure, as seen in clinical studies (1, 40–43). Although variability exists within the diabetic cohort, insulin resistance is present after irradiation, with defects in insulin signaling present in muscle tissue and systemic inflammation. Factors that relate to the risk of diabetes may be the developmental age of the subject at the time of radiation, with smaller, younger primates being at lower risk for metabolic disease later in life, and also experiencing retarded growth and lower adiposity, which may relate to their protected status. Future studies will include continued monitoring of the health of aging, irradiated monkeys to determine if the leaner irradiated monkeys continue to remain disease-free, or if the trend for muscle metabolic defects progresses to eventually overwhelm the ability to dispose of glucose.

ACKNOWLEDGMENTS

This study was supported by the NIH/NIAID through the Radiation Countermeasures Center of Research Excellence (U19 AI67798, P.I. Dr. Nelson Chao, Duke University). The authors are grateful for the valuable contributions from colleagues at RadCCORE and for the donations of irradiated nonhuman primates from our colleagues at the Armed Forces Radiobiology Research Institute, the University of Maryland and the University of Chicago. Additional funding was provided by NIH grants K01 AG033641 and T3OD010946. This work was partially supported by the Department of Radiology Center for Biomolecular Imaging of Wake Forest School of Medicine.

REFERENCES

1. Holmqvist AS, Olsen JH, Andersen KK, de Fine Licht S, Hjorth L, Garwicz S, et al. Adult life after childhood cancer in Scandinavia: diabetes mellitus following treatment for cancer in childhood. Eur J Cancer. 2014; 50:1169–1175. [PubMed: 24507548]
2. van Nimwegen FA, Schaapveld M, Janus CP, Krol AD, Raemaekers JM, Kremer LC, et al. Risk of diabetes mellitus in long-term survivors of Hodgkin lymphoma. J Clin Oncol. 2014; 32:3257–3263. [PubMed: 25154821]
3. Richardson RB. Ionizing radiation and aging: rejuvenating an old idea. Aging (Albany NY). 2009; 1:887–902. [PubMed: 20157573]
4. Hudson MM, Ness KK, Gurney JG, Mulrooney DA, Chemaitilly W, Krull KR, et al. Clinical ascertainment of health outcomes among adults treated for childhood cancer. JAMA. 2013; 309:2371–2381. [PubMed: 23757085]
5. Du Toit DF, Heydenrych JJ, Smit B, Zuurmond T, Louw G, Laker L, et al. The effect of ionizing radiation on the primate pancreas: an endocrine and morphologic study. J Surg Oncol. 1987; 34:43–52. [PubMed: 3543503]
6. DeFronzo RA, Tripathy D. Skeletal muscle insulin resistance is the primary defect in type 2 diabetes. Diabetes Care. 2009; 32(Suppl 2):S157–S163. [PubMed: 19875544]
7. MacVittie TJ, Farese AM, Bennett A, Gelfond D, Shea-Donohue T, Tudor G, et al. The acute gastrointestinal subsyndrome of the acute radiation syndrome: a rhesus macaque model. Health Phys. 2012; 103:411–426. [PubMed: 22929470]
8. Bonora E, Targher G, Alberiche M, Bonadonna RC, Saggiani F, Zenere MB, et al. Homeostasis model assessment closely mirrors the glucose clamp technique in the assessment of insulin sensitivity: studies in subjects with various degrees of glucose tolerance and insulin sensitivity. Diabetes Care. 2000; 23:57–63. [PubMed: 10857969]
9. DeFronzo RA, Tobin JD, Andres R. Glucose clamp technique: a method for quantifying insulin secretion and resistance. Am J Physiol. 1979; 237:E214–E223. [PubMed: 382871]
10. Nguyen-Duy TB, Nichaman MZ, Church TS, Blair SN, Ross R. Visceral fat and liver fat are independent predictors of metabolic risk factors in men. Am J Physiol Endocrinol Metab. 2003; 284:E1065–E1071. [PubMed: 12554597]
11. Fabbrini E, Magkos F, Mohammed BS, Pietka T, Abumrad NA, Patterson BW, et al. Intrahepatic fat, not visceral fat, is linked with metabolic complications of obesity. Proc Natl Acad Sci U S A. 2009; 106:15430–15435. [PubMed: 19706383]
12. Shores NJ, Link K, Fernandez A, Geisinger KR, Davis M, Nguyen T, et al. Non-contrasted computed tomography for the accurate measurement of liver steatosis in obese patients. Dig Dis Sci. 2011; 56:2145–2151. [PubMed: 21318585]
13. Paulino AC, Constine LS, Rubin P, Williams JP. Normal tissue development, homeostasis, senescence, and the sensitivity to radiation injury across the age spectrum. Semin Radiat Oncol. 2010; 20:12–20. [PubMed: 19959027]
14. Brown-Borg HM, Bartke A. GH and IGF1: roles in energy metabolism of long-living GH mutant mice. J Gerontol A Biol Sci Med Sci. 2012; 67:652–660. [PubMed: 22466316]
15. Rincon M, Rudin E, Barzilai N. The insulin/IGF-1 signaling in mammals and its relevance to human longevity. Exp Gerontol. 2005; 40:873–877. [PubMed: 16168602]
16. Nelson OL, Jansen HT, Galbreath E, Morgenstern K, Gehring JL, Rigano KS, et al. Grizzly bears exhibit augmented insulin sensitivity while obese prior to a reversible insulin resistance during hibernation. Cell Metab. 2014; 20:376–382. [PubMed: 25100064]
17. Ramkhelawon B, Hennessy EJ, Menager M, Ray TD, Sheedy FJ, Hutchison S, et al. Netrin-1 promotes adipose tissue macrophage retention and insulin resistance in obesity. Nat Med. 2014; 20:377–384. [PubMed: 24584118]
18. Li X, Wu X, Camacho R, Schwartz GJ, LeRoith D. Intracerebroventricular leptin infusion improves glucose homeostasis in lean type 2 diabetic MKR mice via hepatic vagal and non-vagal mechanisms. PloS One. 2011; 6:e17058. [PubMed: 21379576]

19. Srikanthan P, Karlamangla AS. Relative muscle mass is inversely associated with insulin resistance and prediabetes. Findings from the third National Health and Nutrition Examination Survey. J Clin Endocrinol Metab. 2011; 96:2898–2903. [PubMed: 21778224]
20. Henstridge DC, Bruce CR, Drew BG, Tory K, Kolonics A, Estevez E, et al. Activating HSP72 in rodent skeletal muscle increases mitochondrial number and oxidative capacity and decreases insulin resistance. Diabetes. 2014; 63:1881–1894. [PubMed: 24430435]
21. Hotamisligil GS. Inflammation and metabolic disorders. Nature. 2006; 444:860–867. [PubMed: 17167474]
22. Stubblefield MD. Radiation fibrosis syndrome: neuromuscular and musculoskeletal complications in cancer survivors. PM R. 2011; 3:1041–1054. [PubMed: 22108231]
23. Yarnold J, Brotons MC. Pathogenetic mechanisms in radiation fibrosis. Radiother Oncol. 2010; 97:149–161. [PubMed: 20888056]
24. Baron AD, Tarshoby M, Hook G, et al. Interaction between insulin sensitivity and muscle perfusion on glucose uptake in human skeletal muscle: evidence for capillary recruitment. Diabetes. 2000; 49:768–774. [PubMed: 10905485]
25. Clark MG, Barrett EJ, Wallis MG, Vincent MA, Rattigan S. The microvasculature in insulin resistance and type 2 diabetes. Semin Vasc Med. 2002; 2:21–31. [PubMed: 16222593]
26. Volk BW, Wellmann KF, Lewitan A. The effect of irradiation on the fine structure and enzymes of the dog pancreas. I. Short-term studies. Am J Pathol. 1966; 48:721–753. [PubMed: 5937777]
27. Wellmann KF, Volk BW, Lewitan A. The effect of radiation on the fine structure and enzyme content of the dog pancreas. II. Long term studies. Lab Invest. 1966; 15:100–123. [PubMed: 5911940]
28. El-Assaad W, Buteau J, Peyot ML, Nolan C, Roduit R, Hardy S, et al. Saturated fatty acids synergize with elevated glucose to cause pancreatic beta-cell death. Endocrinology. 2003; 144:4154–4163. [PubMed: 12933690]
29. Poitout V, Amyot J, Semache M, Zarrouki B, Hagman D, Fontés G. Glucolipotoxicity of the pancreatic beta cell. Biochim Biophys Acta. 2010; 1801:289–298. [PubMed: 19715772]
30. DeSesso JM, Jacobson CF. Anatomical and physiological parameters affecting gastrointestinal absorption in humans and rats. Food Chem Toxicol. 2001; 39:209–228. [PubMed: 11278053]
31. Gibbons DL, Spencer J. Mouse and human intestinal immunity: same ballpark, different players, different rules, same score. Mucosal Immunol. 2011; 4:148–157. [PubMed: 21228770]
32. Seok J, Warren HS, Cuenca AG, Mindrinos MN, Baker HV, Xu W, et al. Genomic responses in mouse models poorly mimic human inflammatory diseases. Proc Natl Acad Sci U S A. 2013; 110:3507–3512. [PubMed: 23401516]
33. Akasaki Y, Ouchi N, Izumiya Y, Bernardo BL, Lebrasseur NK, Walsh K. Glycolytic fast-twitch muscle fiber restoration counters adverse age-related changes in body composition and metabolism. Aging Cell. 2014; 13:80–91. [PubMed: 24033924]
34. Wagner JE, Kavanagh K, Ward GM, Auerbach BJ, Harwood HJ Jr, Kaplan JR. Old world nonhuman primate models of type 2 diabetes mellitus. ILAR J. 2006; 47:259–271. [PubMed: 16804200]
35. Harwood HJ Jr, Listrani P, Wagner JD. Nonhuman primates and other animal models in diabetes research. J Diabetes Sci Technol. 2012; 6:503–514. [PubMed: 22768880]
36. Kavanagh K, Fairbanks LA, Bailey JN, Jorgensen MJ, Wilson M, Zhang L, et al. Characterization and heritability of obesity and associated risk factors in vervet monkeys. Obesity (Silver Spring). 2007; 15:1666–1674. [PubMed: 17636084]
37. Wagner JD, Jayo MJ, Bullock BC, Washburn SA. Gestational diabetes mellitus in a cynomolgus monkey with group A streptococcal metritis and hemolytic uremic syndrome. J Med Primatol. 1992; 21:371–374. [PubMed: 1307756]
38. Saisho Y, Manesso E, Butler AE, Galasso R, Kavanagh K, Flynn M, et al. Ongoing beta-cell turnover in adult nonhuman primates is not adaptively increased in streptozotocin-induced diabetes. Diabetes. 2011; 60:848–856. [PubMed: 21270238]
39. Hansen BC, Newcomb JD, Chen R, Linden EH. Longitudinal dynamics of body weight change in the development of type 2 diabetes. Obesity (Silver Spring). 2013; 21:1643–1649. [PubMed: 23713008]

40. Baker KS, Chow EJ, Goodman PJ, Leisenring WM, Dietz AC, Perkins JL, et al. Impact of treatment exposures on cardiovascular risk and insulin resistance in childhood cancer survivors. Cancer Epidemiol Biomarkers Prev. 2013; 22:1954–1963. [PubMed: 24008489]

41. de Vathaire F, El-Fayech C, Ben Ayed FF, Haddy N, Guibout C, Winter D, et al. Radiation dose to the pancreas and risk of diabetes mellitus in childhood cancer survivors: a retrospective cohort study. Lancet Oncol. 2012; 13:1002–1010. [PubMed: 22921663]

42. Oeffinger KC, Sklar CA. Abdominal radiation and diabetes: one more piece in the puzzle. The Lancet Oncology. 2012; 13:961–962. [PubMed: 22921662]

43. Wang GJ, Li XK, Sakai K, Lu Cai. Low-dose radiation and its clinical implications: diabetes. Hum Exp Toxicol. 2008; 27:135–142. [PubMed: 18480138]

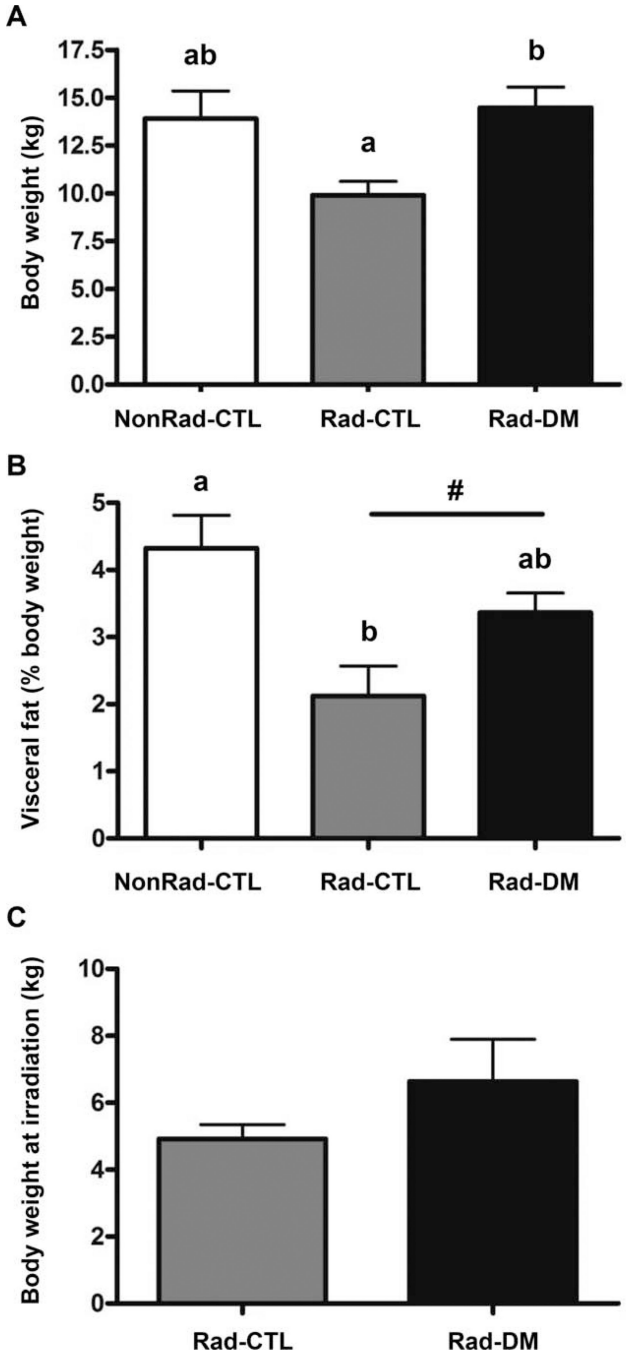

FIG. 1.

Panel A: Body weights were recorded in three groups of rhesus macaques at the time of assessment: nonirradiated nondiabetic (NonRad-CTL; n = 12); 7–8 years post exposure, irradiated nondiabetic (Rad-CTL; n = 22); and irradiated diabetic (type 2) (Rad-DM; n = 9) (ANCOVA, $P < 0.001$). Unlike letters denote significance between groups with $P < 0.05$. Panel B: Percentage of total body weight that was attributed to the visceral fat depot, as assessed by computed tomography (ANCOVA, $P = 0.004$). Unlike letters denote significance between groups with $P < 0.05$. A significant effect of prior irradiation was

indicated by the "#" ($P = 0.004$). Panel C: Body weights at the time of irradiation, 7–8 years prior to the assessment time point (ANOVA, $P = 0.10$).

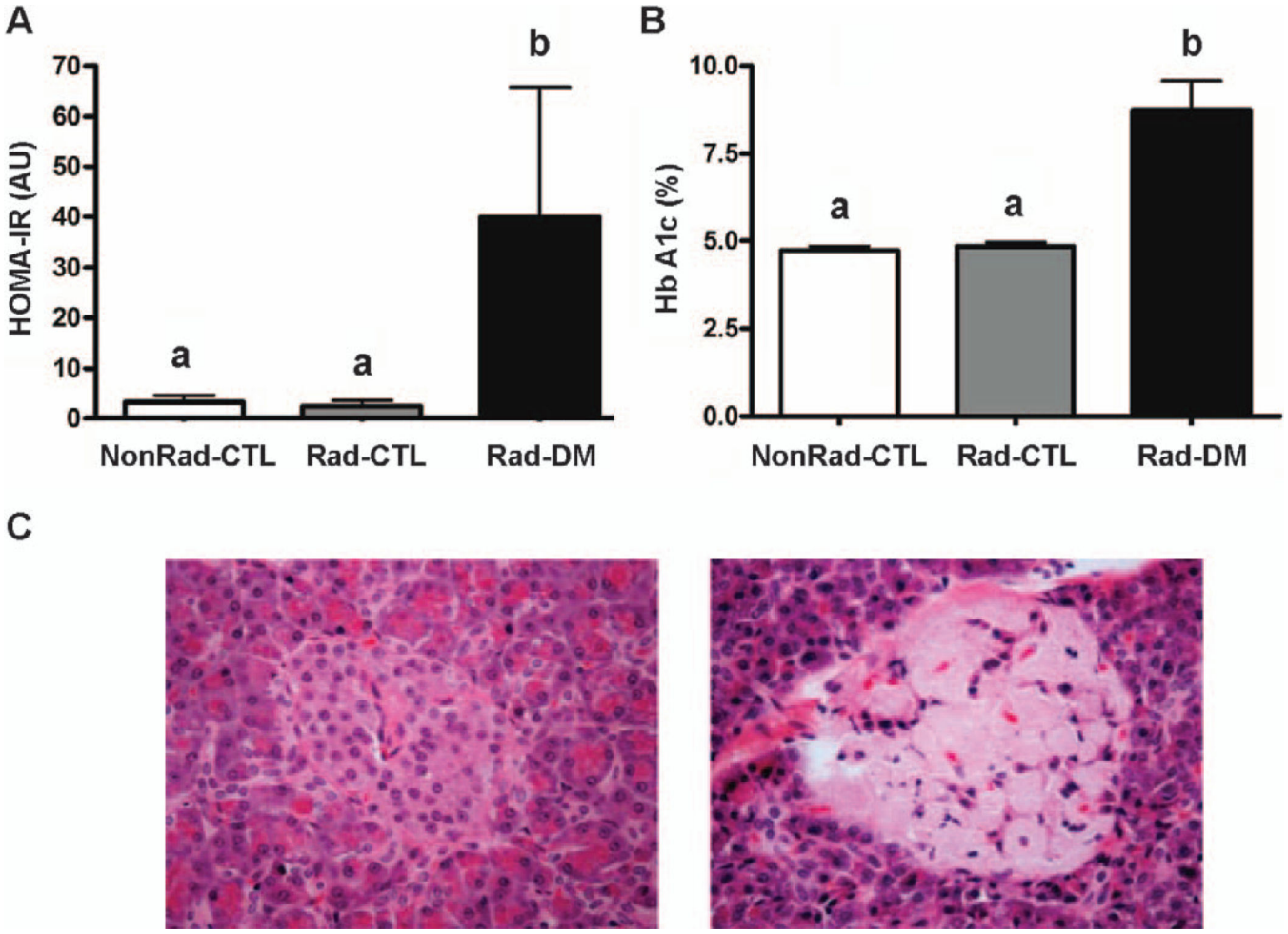

FIG. 2.

Panel A: Homeostasis model assessment index for insulin resistance (HOMA-IR) in nonirradiated nondiabetic (NonRad-CTL; n = 12), irradiated nondiabetic (Rad-CTL; n = 22) and irradiated diabetic (type 2) (Rad-DM; n = 9) rhesus macaques (ANOVA, $P < 0.001$). Unlike letters denote significance between groups with $P < 0.05$. Panel B: Average glycation of hemoglobin chain A1c (Hb A1c) (ANOVA, $P = 0.001$). Unlike letters denote significance between groups with $P < 0.05$. Panel C: Histopathology of a pancreatic islet from two Rad-DM monkeys that died years after irradiation and one NonRad-CTL monkey (20× magnification). The left side panel shows a normal appearing islet and beta cells from one diabetic monkey, and the right side panel shows an islet from another diabetic animal with significant amyloid deposition and loss of beta cells.

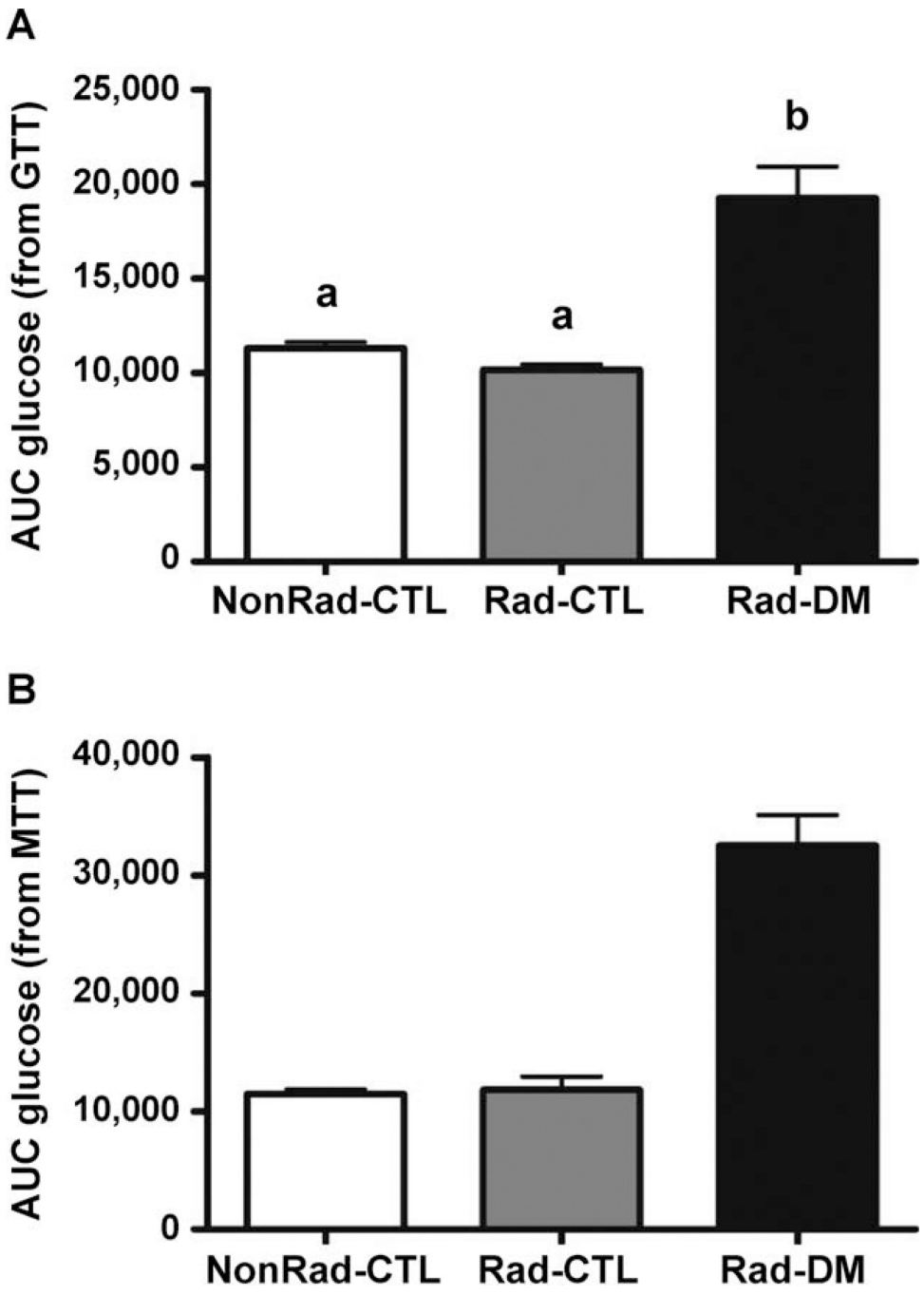

FIG. 3.

Areas under the curve (AUC) for (panel A) glucose after glucose tolerance testing (GTT) and (panel B) meal tolerance testing (MTT) in nonirradiated nondiabetic (NonRad-CTL), irradiated nondiabetic (Rad-CTL) and irradiated diabetic (type 2) (Rad-DM) rhesus macaques. ANOVA for AUC from GTT, $P < 0.001$ and for MTT, $P = 0.06$. n = 6/group. Unlike letters denote significance between groups with $P < 0.05$.

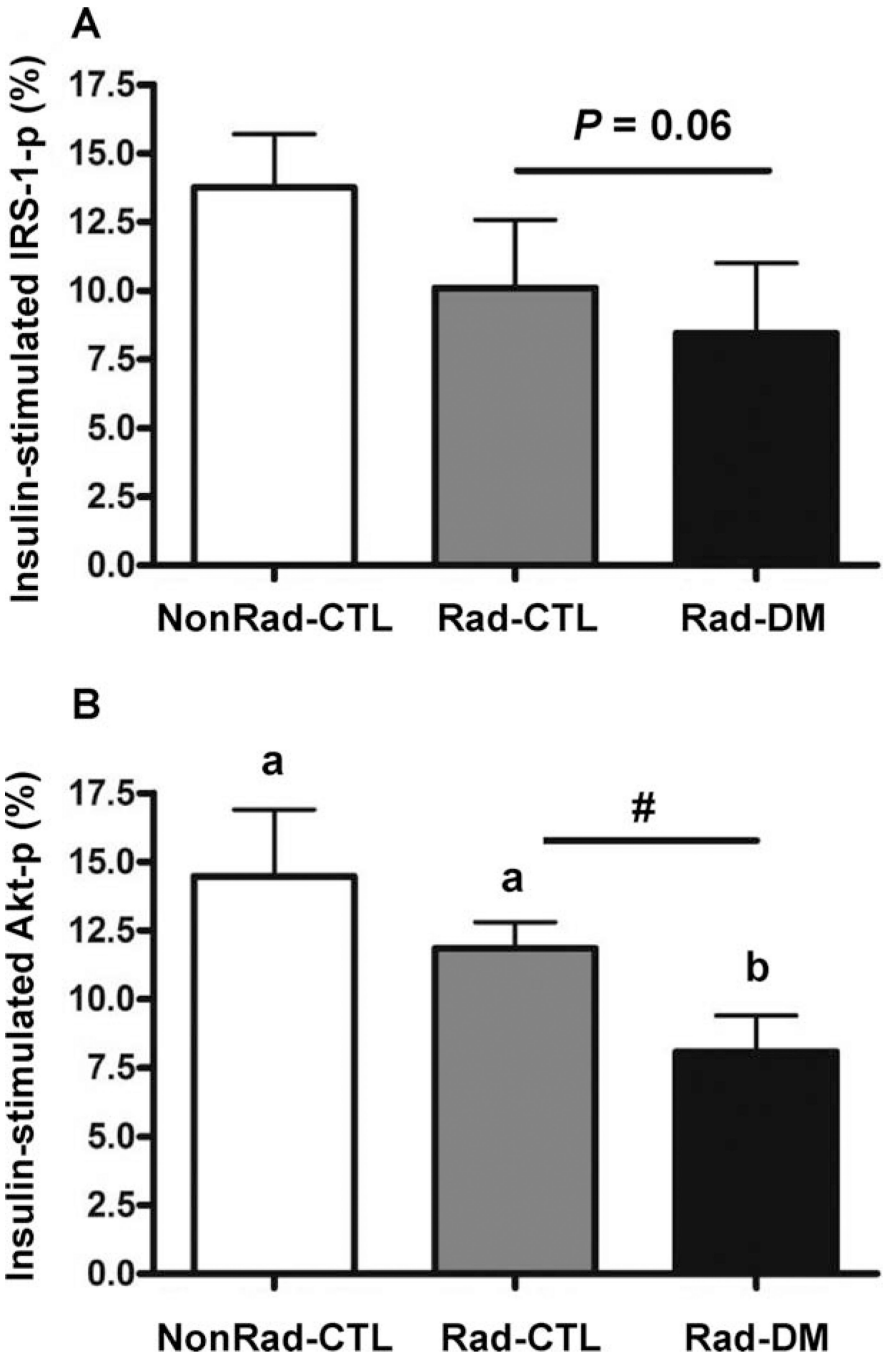

FIG. 4.

Activation of insulin signaling proteins downstream of the insulin receptor in skeletal muscle after insulin infusion in nonirradiated nondiabetic (NonRad-CTL), irradiated nondiabetic (Rad-CTL) and irradiated diabetic (type 2) (Rad-DM) rhesus macaques (n = 6/group). Panel A: Activation of IRS-1 had a trend towards reduction with prior irradiation ($P = 0.06$). Overall ANOVA, $P = 0.07$. Panel B: Activation of Akt was significantly reduced in monkeys with prior irradiation (ANOVA, $P = 0.03$), and irradiated diabetic monkeys had significantly worse activation post-insulin stimulation than both nondiabetic groups. A

significant effect of prior irradiation was indicated by the "#" (ANOVA, $P = 0.05$). Unlike letters denote significance between groups with $P < 0.05$.

TABLE 1

Demographic Information, Cardiometabolic and Inflammatory End Points for Nonirradiated Nondiabetic (NonRad-CTL; n = 12), Irradiated Nondiabetic (Rad-CTL; n = 22) and Irradiated Diabetic (Type 2) (Rad-DM; n = 9) Rhesus Macaques

	NonRad-CTL	Rad-CTL	Rad-DM	ANOVA (*P*)	Radiation effect (*P*)
Age at assessment (years)	11.3 (0.3)	11.4 (0.6)	12.6 (1.2)	0.32	N/A
Age at exposure (years)	N/A	4.0 (0.43)	5.0 (0.77)	0.23	N/A
Irradiation dose (Gy)	N/A	7.43 (0.14)^a	7.00 (0.20)^b	<0.001	N/A
Glucose (mg/dL)	69.6 (4.8)^a	62.8 (3.0)^a	200.1 (27.9)^b	<0.001	<0.001
Insulin (lIU/mL)	19.1 (8.2)	15.0 (7.4)	46.0 (26.0)	0.11	0.42
Total plasma cholesterol (mg/dL)	163 (10.4)	179 (8.5)	208 (30.2)	0.24	0.21
Triglycerides (mg/dL)	85.1 (22.5)^a	64.9 (9.1)^a	543 (268)^b	<0.001	0.12
Systolic blood pressure (mmHg)	140 (5.1)	143 (6.5)	135 (8.1)	0.75	0.98
Diastolic blood pressure (mmHg)	74.9 (3.1)	73.7 (2.0)	72.7 (2.3)	0.84	0.61
Pulse wave velocity (m/s)	10.5 (0.68)	10.8 (1.04)	10.3 (0.59)	0.92	0.91
Heart rate (bpm)	126 (4.1)	136 (3.9)	132 (5.0)	0.20	0.09
C-reactive protein (ng/mL)*	21.0 (7.2)	25.7 (6.6)	33.1 (5.7)	0.43	0.30
Interleukin-6 (pg/mL)*	622 (315)	479 (124)	359 (100)	0.44	0.30
MCP-1 (pg/mL)	331 (33.0)^a	444 (28.9)^b	479 (36.9)^b	0.02	0.005

^{a,b}Unlike letters denote significance between groups with $P < 0.05$.

*n = 6/group.

TABLE 2

Body Composition Analysis by Computed Tomography of Nonirradiated Nondiabetic (NonRad-CTL; n = 12), Irradiated Nondiabetic (Rad-CTL; n = 22) and Irradiated Diabetic (Type 2) (Rad-DM; n = 9) Rhesus Macaques

	NonRad-CTL	Rad-CTL	Rad-DM	ANCOVA (*P*)	Radiation effect (*P*)
BMI (kg/m^2)*	43.3 (4.7)	34.0 (2.9)	45.6 (2.6)	0.07	0.48
Waist circumference (cm)*	44.6 (4.4)	36.6 (3.7)	45.8 (3.2)	0.21	0.50
Trunk length (cm)	40.9 (0.72)^a	37.7 (0.49)^b	38.3 (1.09)^b	0.006	0.001
Liver attenuation (HU)	58.7 (1.8)^a	65.2 (2.7)^b	54.9 (4.6)^{a,b}	0.009	0.03
Muscle attenuation (HU)	65.4 (1.1)	68.4 (1.6)	67.1 (1.7)	0.30	0.16
Total body fat (% BW)	18.3 (1.7)^a	11.6 (1.6)^b	21.1 (2.4)^a	0.004	0.24
Total body lean tissue (% BW)	57.8 (3.0)^a	72.8 (2.5)^b	57.4 (2.8)^a	0.0005	0.03
Fat mass (kg)	2.86 (0.39)^a	1.06 (0.38)^b	3.01 (0.48)^a	0.004	0.07
Lean mass (kg)	7.89 (0.26)^a	6.11 (0.25)^b	7.94 (0.32)^a	0.00002	0.01
Visceral:subcutaneous abdominal fat	2.57 (0.20)^a	2.06 (0.24)^{a,b}	1.34 (0.18)^b	0.007	0.006
Abdominal subcutaneous fat (% BW)	1.83 (0.003)	1.25 (0.003)	3.25 (0.01)	0.09	0.70
Fat:lean tissue, legs only	0.28 (0.043)^a	0.15 (0.023)^b	0.32 (0.037)^a	0.007	0.15
Total leg lean tissue (% BW)	16.5 (0.90)^{a,c}	21.0 (0.65)^b	15.33 (0.84)^{b,c}	0.00008	0.07
Total leg fat tissue (% BW)	3.74 (0.34)^a	2.61 (0.30)^b	4.10 (0.037)^a	0.015	0.22

^{a,b,c}Unlike letters denote significance between groups with $P < 0.05$.

*n = 6/group.

TABLE 3

Calculated Indices of Glucose Metabolism from Glucose and Meal Tolerance Testing

	NonRad-CTL	Rad-CTL	Rad-DM	ANOVA (*P*)	Radiation effect (*P*)
Disposition index	8.46 (3.46)	7.26 (2.51)	10.6 (3.79)	0.77	0.91
Acute insulin response	74.38 (19.7)	75.1 (33.4)	80.8 (10.6)	0.99	0.93
K value for glucose disappearance	1.28 (0.33)	1.30 (0.39)	0.52 (0.13)	0.15	0.36
Post-meal triglyceride (mg/dL)	98.9 (24.4)^{a}	61.6 (12.4)^{a}	606 (300)^{b}	0.001	0.34
AUC insulin glucose tolerance testing	4,754 (1,379)	3,816 (2,266)	5,114 (2,734)	0.92	0.93
AUC insulin meal tolerance testing	7,339 (1,590)	11,722 (3,254)	11,853 (4,622)	0.63	0.36

Notes. n = 6/group. AUC = area under the curve.

^{a,b}Unlike letters denote significance between groups with $P < 0.05$.